Cubic-to-tetragonal phase transition in $RbCaF_3$ investigated by diffraction experiments with neutrons, x rays, and γ rays from a Mössbauer source

H. Jex, J. Maetz, and M. Müllner
Institut für Kernphysik der J. W. Goethe - Universität, D-6000 Frankfurt, Germany
(Received 13 April 1979)

The cubic-to-tetragonal phase transition of $RbCaF_3$ at $T_0 = 198$ K has been studied on single crystals and powder samples utilizing diffraction techniques with various types of radiation. From our x-ray experiments we have determined the temperature dependence of the domain distribution. In particular an anisotropic distribution of domains was found close above T_0. The neutron-diffraction data obtained from powder samples were taken to extract the critical exponent β free from the influence of domains. We find $\beta = 0.25(1)$. We show that the bond lengths of the Ca–F bond exhibit a pronounced minimum at the transition. The fluctuations of the order parameter $(\langle\varphi^2\rangle - \langle\varphi\rangle^2)^{0.5}$ are compared with $\langle\varphi\rangle$ to determine the critical region below T_0. A peak in $\langle\varphi^2\rangle$ is found for the first time in the neutron experiments. The Mössbauer γ-ray-diffraction experiments were performed in order to separate elastic and inelastic scattering components from the central peak above T_0 and from the superlattice point $\frac{1}{2}(311)_{\text{cubic}}$ below T_0 with an energy resolution of 60 neV.

I. INTRODUCTION

$RbCaF_3$ belongs to the group of perovskites which undergo an antiferrodistortive phase transition from a cubic to a tetragonal phase which is connected with the softening of a triply degenerate Γ_{25} phonon at the R point of the cubic Brillouin zone. The soft mode consists of alternative rotations of the CaF_6 octahedrons around one of the [100] axes. At the phase transition the space group changes from cubic O_h^1 ($Pm3m$) to tetragonal D_{4h}^{18} ($I4/mcm$). Different T_0 values have been reported [193,[1] 197,[2] and 198 K (Ref. 3)].

The order parameter of the transition is the staggered rotation angle $\langle\varphi\rangle$ of the CaF_6 octahedrons which is proportional to the displacements of the fluorine atoms from their high-temperature sites. There is no privileged cubic axis and no predetermination which of them becomes the tetragonal one after the phase transition; therefore the crystal decays into three orthogonal domains. These domains, which have been observed visually by Modine *et al.*,[4] cause considerable difficulties in the optical birefringence and the EPR experiments,[4] in ultrasound experiments and Brillouin scattering,[5] and in x ray and neutron scattering on single crystals.[6] Therefore, in such structural phase transitions, powder experiments are useful since the results are free from domain effects. Ridou *et al.*[7] investigated some structural data applying x-ray diffraction on powder samples. The lattice vibrations of $RbCaF_3$ have been measured by Rousseau *et al.*[8] with inelastic neutron scattering from single crystals, and detailed investigations of the soft mode and the central peak have been published. These neutron experiments were done by Kamitakahara *et al.*[9] and by Almairac *et al.*[1]

We contribute in this article results from our experiments utilizing three different types of diffraction experiments which elucidate some new aspects concerning the upper phase transition in $RbCaF_3$.

Neutron diffraction from powder samples was performed to investigate the structural parameters free from domains and extinction. Applying profile analysis of the spectra due to Rietveld,[10] we determined the bifurcation of the lattice constants and from the position of the fluorine atoms the order parameter $\langle\varphi\rangle$. The anisotropic mean-square vibrational amplitudes of the ions are given. From these experimental data we evaluate the order-parameter fluctuations which define the critical-temperature region below T_0 from $\langle\varphi\rangle < \langle\varphi^2\rangle^{0.5}$ experimentally. Our neutron experiments showed for the first time a peak in the Debye-Waller factor of the fluorines which must be related to the enhanced fluctuations at the phase transition. Also the bond length between Ca–F was determined, indicating a pronounced anomaly which indirectly shows deformation of the electronic shells. Our x-ray-diffraction experiments described in the third chapter were mainly done with the aim to investigate the domain distribution in single crystals. Especially we measured the temperature dependence of the domain volumes and we discuss the consequences on measurements of the critical exponent β from single-crystal data.

Finally, we apply Mössbauer diffraction of ^{57}Co γ rays in $RbCaF_3$ in order to separate elastic and inelastic scattering from the central component with an en-

ergy resolution of $dE = 60$ neV. Our data are compared with the neutron work by Kamitakahara *et al.*[9] and by Almairac *et al.*[1] using three-axis neutron spectrometers with an energy resolution of the order of 0.165 meV. We also measured the elastic and inelastic parts of the superlattice reflection $\frac{1}{2}(311)_{\text{cubic}}$ below T_0 with the high-energy resolution.

II. NEUTRON POWDER DIFFRACTION

In our neutron experiments on $RbCaF_3$, we measrured the powder-diffraction patterns at the FR2 reactor, Karlsruhe. The probe container was a thin-walled cylindrical vanadium can of 2-cm diameter and 5-cm height. The sample was cooled with a closed-cycle He refrigerator from room temperature to 60 K with an accuracy of the temperature settings of ± 0.5 K. The temperature gradient along the probe is of the same order. The diffraction paterns measured with an incident wavelength of $\lambda = 1.0156(2)$ Å were collected from a scattering range of $10° < 2\theta < 105°$ covering up to 202 reflections in the tetragonal phase. Structure parameters and anisotropic temperature factors were refined by means of profile analysis[10] of the experimental data corrected for absorption.[11] Preliminary results have been published in a short note by Maetz *et al.*[12]

From the experiments we deduce several relevant structure parameters. Figure 1 presents the order parameter $\langle\varphi\rangle$ and the order-parameter fluctuations $\langle\varphi^2\rangle^{0.5}$ determined from the positions of the fluorines and their mean-square vibrational amplitudes, respectively. The order parameter can be fitted to a law $\langle\varphi\rangle = \varphi_0(T_0 - T)^\beta$ with $\beta = 0.25(1)$, $T_0 = 197(1)$ K, and $\varphi_0 = 2.24(3)°$. This result agrees with a twisting angle of $\langle\varphi\rangle = 7.1^0$ at 77 K deduced from V_k-center EPR spectra measured by Halliburton *et al.*[13]; we obtain 7.4°. We recall that the rotation angle $\langle\varphi(T=0)\rangle = \varphi_0 T_0^\beta = 8.4°$ would be about a factor of four larger than in $SrTiO_3$. A value of $\beta = 0.25$ has been reported by Modine *et al.*[4] in a temperature range $187 < T < 197$ K. Very recent EPR data by Buzare *et al.*[22] give $\beta = 0.18(2)$ between $190 < T < 195.3$ K, while the birefringence results by Kleemann *et al.*[14] are $\beta = 0.28(1)$ in the range $193.6 < T < 196.5$ K.

From Fig. 1 we estimate the critical region where the fluctuations exceed the order parameter $\langle\varphi^2\rangle^{0.5} > \langle\varphi\rangle$ to extend below T_0 down to about 180 K. Since the majority of data are from lower temperatures than $T_0 - 15$ K, we are in a region where fluctuation corrections may be neglected. Nevertheless, we would like to point out that our temperature exponent β is quite consistent with the above experiments which have been concentrated to $T_0 - T \to 0$. Our experiments were not extended to lower temperatures than 60 K because $RbCaF_3$ undergoes two more phase transitions below 50 K as shown by the Raman-scattering study by Rushworth *et al.*[15]

Figure 2 presents the tetragonal splitting of the lattice constants. At the bifurcation point the cell volume seems to remain a smooth function. These results agree with the x-ray powder data by Ridou *et al.*[7] However, very recent investigations by Ridou *et al.*,[16] using a double-crystal x-ray-diffraction technique with a more accurate temperature setting showed a discontinuity of 10^{-3} Å in the lattice constant indicating the weak first-order character of the phase transition. Since we independently determined the splitting of the lattice constants $(c-a)/a$ and the order parameter $\langle\varphi\rangle$ from the profile analysis, we are able to check the relation $(c-a)/a = 1.5\langle\varphi\rangle^2$, which was derived by Rousseau *et al.*[17] under the assumption of constant volume and rigid CaF_6 octahedrons. Our results in Fig. 3 show that this law does not

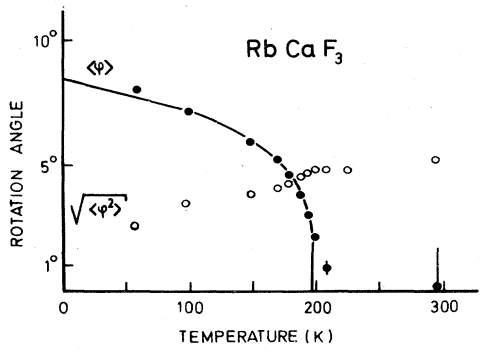

FIG. 1. Temperature dependence of the order parameter $\langle\varphi\rangle$ and its fluctuations $\langle\varphi^2\rangle^{0.5}$. The theoretical full line represents the law $\langle\varphi\rangle = 2.24(197-T)^{0.25}$.

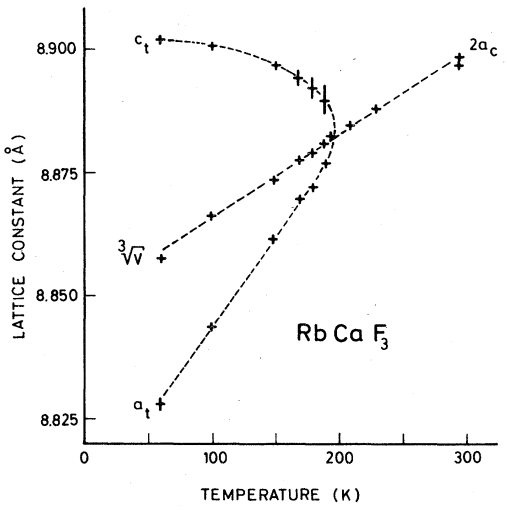

FIG. 2. Tetragonal splitting of the lattice constants in $RbCaF_3$. Broken lines are only guides for the eye.

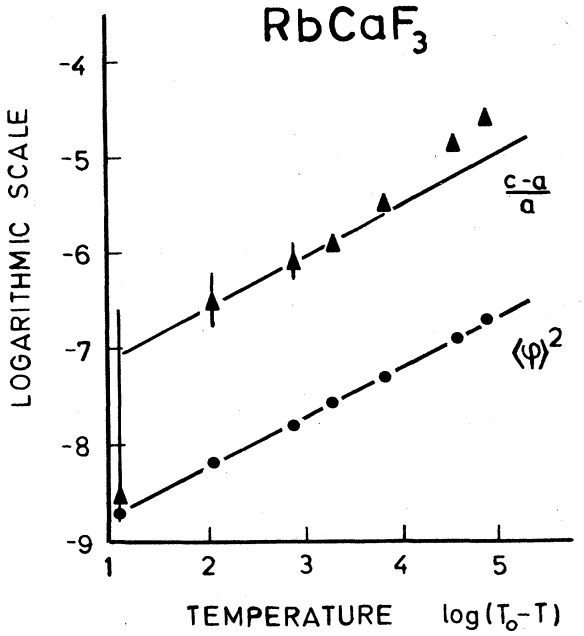

FIG. 3. Lattice-constant splitting $(c-a)/a$ (▲) and square of the order parameter $\langle\varphi\rangle^2$(●) of $RbCaF_3$ in a log-log plot vs temperature. Error bars are given whenever they surmount the size of the symbols. The full lines represent the power law with exponent $2\beta=0.5$ for comparison.

hold, because these assumptions are not fulfilled satisfactorily. A unique power law for the lattice constants splitting as a function of temperature seems to be not so well defined in the investigated temperature range as a power law for the order parameter $\langle\varphi\rangle$.

An important structural quantity in this perovskite lattice is the Ca–F bond length, which varies considerably at the phase transition, when the CaF_6 octahedrons start to move out form their cubic equilibrium positions. Considering one CaF_6 unit, we have in the tetragonal phase four fluorine neighbors in the plane of rotation having the same distance to the central Ca atom. The two fluorine neighbors lying in the rotation axis define a second bond-length distance among the nearest neighbors in the tetragonally distorted phase. Figure 4 presents our data. In the cubic phase the bond lengths to all six neighbors are equal and become smaller as we go down from room temperature to the transition point in accord with the thermal-expansion coefficient. However, below the transition temperature the bond length in the rotational plane increases again with the gradual rotation of the CaF_6 octahedrons, as well as the bond length in the rotational axis grows due to the gradual increase of the tetragonal c axis of the elementary cell. We recall that the bond length in CaF_2 crystals is about 2.365 Å compared with the minimum of 2.221 Å in $RbCaF_3$. The pronounced minimum of the

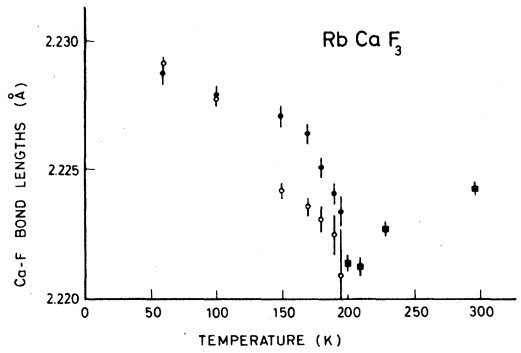

FIG. 4. Ca–F bond-length variation across the phase transition of $RbCaF_3$. In the tetragonal phase full dots represent lengths in the plane of rotation of the CaF_6 octahedrons, while open dots are representative of the Ca–F distance in the rotation axis.

bond length at the transition point means that a strong additional deformation of the electronic shells is expected to take place at this temperature on the fluorines rather than the calcium ions. One further concludes that the octahedral configuration of CaF_6 remains rather stable in shape but it is not rigid. This stems from the fact that the bond lengths of the tetragonal phase do not differ significantly.

From the profile analysis of our data we determined the anisotropic mean-square vibrational amplitudes $\langle u^2\rangle$ which are presented in Fig. 5 in terms of crystallographic B factors ($B=8\pi^2\langle u^2\rangle$) of the individual ions. Due to the point symmetry of the ion positions in the cubic structure, the vibrational tensors are represented by spheres in the case of rubidium and calcium, while fluorine becomes an ellipsoid of revolution [$B_{11}(F)=B_{22}(F)$ and $B_{33}(F)$]. Below the transition we maintain this as a pseudocubic approach in the Rietveld data analysis due to the smallness of the tetragonal splitting. Figure 5 shows the large anisotropy of the fluorine vibrational amplitudes. $B_{11}(F)=B_{22}(F)$ may be related to the rota-

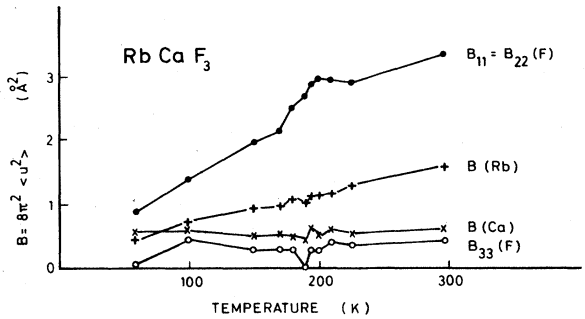

FIG. 5. Individual mean-square vibrational amplitudes of the ions of $RbCaF_3$ in terms of crystallographic B values. Full lines are only guides for the eye.

tional angle of the CaF_6 octahedrons via

$$B_{11}(F)=8\pi^2\langle u_1^2(F)\rangle=8\pi^2(\tfrac{1}{2}a)^2\langle\varphi^2\rangle \ ,$$

where a is the lattice constant. At room temperature we obtain $\langle\varphi^2\rangle^{0.5}\cong 5°$; this corresponds approximately to the free space between the ionic radii in that structure. The mean-square vibrational amplitudes start to freeze in at the phase transition.

We would also like to point out here that $B_{11}(F)=B_{22}(F)$ shows a pronounced enhancement at the phase-transition temperature, while the other B values — $B_{33}(F)$ included — are smooth within the error bars. A peak in the mean-square vibrational amplitudes was predicted theoretically by Meissner *et al.*[18] We shall come to this point in more detail in the discussion.

III. X-RAY-DIFFRACTION EXPERIMENTS

The x-ray experiments were performed on single crystals with the aim of studying the influence of domains below the phase transition. As we pointed out in the introduction, there are three orthogonal domain orientations expected from symmetry considerations. At the phase transition the space group changes from $O_h^1(Pm3m)$ to $D_{4h}^{18}(I4/mcm)$; however, with regard to our measuring procedure, we favor in this chapter a pseudocubic notation in the space group $D_{4h}^{12}(P4_2/mbc)$. In this description the superlattice reflections below T_0 are characterized by Miller indices (h,k,l) with the restriction h, k, and l are odd and h is unequal to k.

The measurements were done on a conventional four-circle x-ray diffractometer furnished with a molybdenum tube and a graphite monochromator. It was proved experimentally that there were no contaminations of the half wavelength which is necessary for studying superlattice structure reflections. The crystal was cooled by an electronically controlled cold air blast in the temperature range from 235 to 123 K. At the beginning and at the end of each measurement the temperature was controlled by a thermocouple element in the position of the crystal. The accuracy of the temperature setting was ± 1 K. After each temperature change the orientation matrix was refined. The full set of pseudocubic, symmetrically equivalent reflections with $2\theta < 24°$ was measured. Due to the slightly ellipsoidal shape of the crystal — its averaged spherical diameter was 0.3 mm — an absorption correction corresponding to each orientation was applied. The mosaic spread was smaller than 0.15°.

For an extraction of the relative domain volumes from the single-crystal experiments, those superlattice points with two equal indices $k=1$ are well suited. Taking the measured intensities of all their symmetrically equivalent superlattice structure reflections, the relative domain volumes may be evaluated as follows. The relative volume V_a of the domains with their tetragonal axis parallel to the a axis of the cubic crystal is

$$V_a=1-\frac{2I_{hll}}{I_{hll}+I_{lhl}+I_{llh}}; \quad l\neq h \ .$$

I_{hll} is the sum of intensities of the eight reflections $(\pm h, \pm l, \pm l)$. The domain volumes V_b and V_c are similarly determined; the normalization $V_a+V_b+V_c=1$ holds. The resulting intensities obtained from (311) and (133) reflections are plotted in Fig. 6. The data show that domains already exist above the phase-transition temperature T_0. In this temperature range Almairac *et al.*[1] investigated a central peak and an overdamped soft mode. The anisotropy of the scattered intensity in our measurment may be explained by a structural disorder starting in the cubic phase. It is an indication that domain scattering which should be elastic is part of the central component. Cooling the crystal below the phase transition, the relative domain volumes vary; one branch increases, two branches decrease. Consequently, if experiments are sensitive to the domain structure, an additional temperature effect is produced. We also emphase that the domains are nevertheless almost equally distributed at their birth; $V_a=V_b=V_c=0.33$ roughly holds.

We recall that the rotational displacement $\langle\varphi\rangle$ of the CaF_6 octahedrons, which is the order parameter of the phase transition, can be determined from this experiment. In view of the domains, the x-ray intensities were averaged over the full set of equivalent reflections. Then we used the following procedure to

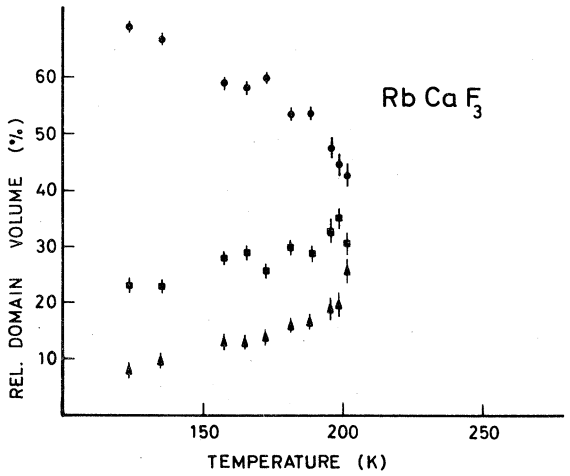

FIG. 6. Relative domain volumes of $RbCaF_3$ as a function of temperature. The symbols represent V_c (●), V_b (■), and V_a (▲).

evaluate $\langle\varphi\rangle$. The intensity ratio of the (311) and (222) reflections and respectively, of the (133) and (420) reflections, were evaluated numerically from the structure factors as a function of $\langle\varphi\rangle$. The experimental ratio of the averaged intensities was compared with the gauge curve. It was checked that extinction does not contribute. The angular distance in the scattering of the compared reflections is so small that the temperature factors or the angular-dependent absorption cannot falsify the rotational displacement $\langle\varphi\rangle$. Proceeding this way, the domains do not influence the determination of $\langle\varphi\rangle$. The results are shown in Fig. 7. The data are fitted by a temperature law $\langle\varphi\rangle=\varphi_0(T_0-T)^\beta$ with $\beta=0.25(1)$, $\varphi_0=2.47(2)°$, and $T_0=199(1)$ K. The deviation near T_0 between theory and experiment and the values in the cubic phase can be attributed to the scattering from the central peak and the soft mode. The exponent $\beta=0.25$ seems to hold beyond the critical region towards lower temperatures when a domain-free analysis is applied. This was achieved here by averaging over the symmetry-equivalent Bragg reflections. The rotation-angle parameter φ_0 deviates about 10% from the neutron-powder value. Perhaps the penetration depth of the radiation is important; we estimate 70 μm in the case of the (311) superlattice point for our x rays. Thus the enhancement may be due to surface effects.

Figures 8(a) and 8(b) pictures the influence of the temperature-dependent domains on the averaged intensities of the superlattice reflections $(I_{311},I_{131},I_{113})$ and $(I_{133},I_{313},I_{331})$ in D_{4h}^{13} notation. For small rotation $\langle\varphi\rangle$ the intensities of the superlattice reflections should be proportional to the square of the rotational displacement. Therefore, having in mind $\beta=0.25$, the squared intensities are expected to depend linearly on the temperature. In Fig. 8 it is evident that the total intensity $I_{tot}^2=(I_{hll}+I_{lhl}+I_{llh})^2$ — but not the intensities of the single groups — follow the power

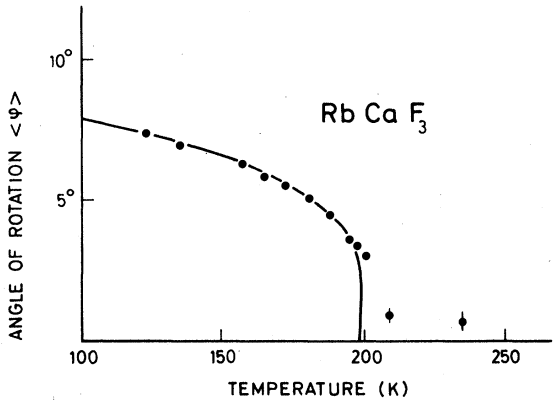

FIG. 7. Order parameter $\langle\varphi\rangle$ from x-ray measurements on a single crystal. The theoretical curve represents the law $\langle\varphi\rangle=2.47(199-T)^{0.25}$.

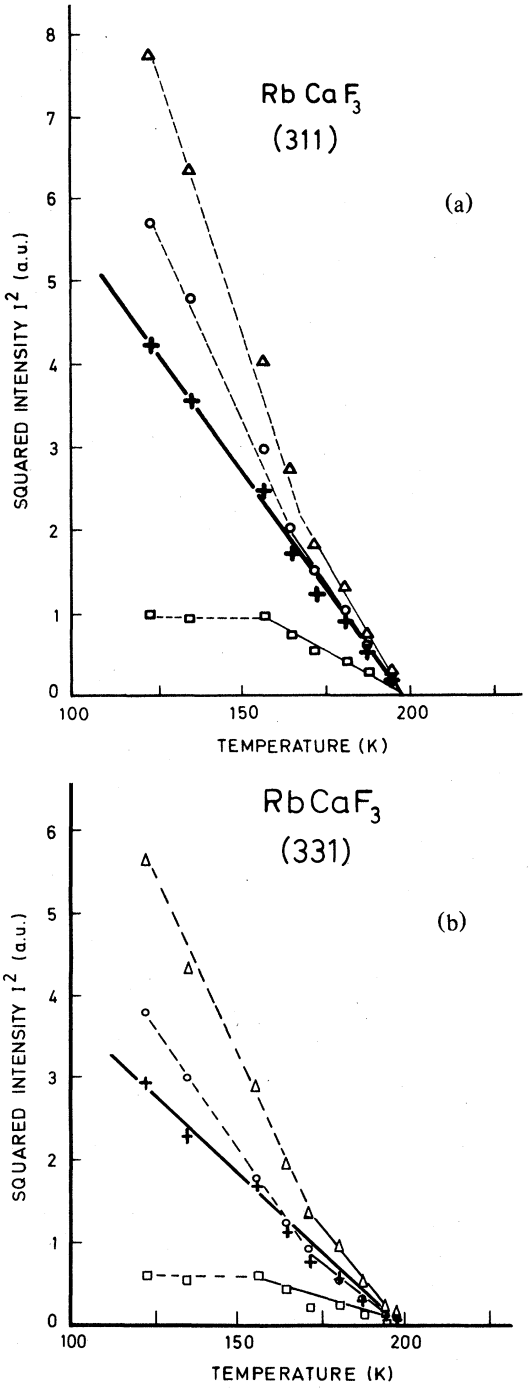

FIG. 8. (a) Intensity of the (311) reflections (in D_{4h}^{13} notation) averaged over $(\pm h,\pm k,\pm l)$. The following symbols are chosen I_{311}^2 (Δ), I_{131}^2 (○), I_{113}^2 (□), and $\frac{1}{9}I_{tot}^2$ (+), where $I_{tot}=I_{311}+I_{131}+I_{113}$. The full line represents the power law $I^2\propto(T_0-T)$; deviations are marked by dashed lines. (b) Intensity of the (331) reflections (in D_{4h}^{13} notation) averaged over $(\pm h,\pm k,\pm 1)$. The following symbols are chosen I_{331}^2 (Δ), I_{313}^2 (○), I_{133}^2 (□), and $\frac{1}{9}I_{tot}^2$ (+). The full and broken lines have the same meaning as in (a).

law $I^2 \propto (T_0 - T)$. For a single group we have instead

$$I_{hll} = \tfrac{1}{2}(V_b + V_c) I_{\text{tot}} \ ,$$

which clearly shows that the temperature-dependent variation of domain volumes generates an additional temperature contribution. Above T_0, deviations are registrated due to the central peak which contains, for instance, inelastic contributions from the overdamped unresolved soft mode. However, below T_0 we recognize that there are two regions in the I^2_{hll} ($h \neq 1$) data, which correspond roughly to the range of large and negligable fluctuations ($\langle\varphi^2\rangle^{0.5} \gtrsim \langle\varphi\rangle$). We realize that in the region of large fluctuations the same power law seems to hold, while at low temperatures the data of I^2_{hll} switch off. Critical scattering, which has not been subtracted here, will not disturb the intensity relations among the reflection groups which are governed by the domain volumes.

IV. MÖSSBAUER-DIFFRACTION EXPERIMENTS

Fundamental investigations of the central component present at structural phase transitions have been performed applying inelastic neutron scattering in the perovskite structure, e.g., by Shapiro *et al.*[19] Also the high-energy resolution of γ rays from a ^{57}Co Mössbauer source — with natural linewidth 4.6 neV — has effectively been utilized for the separation of the elastic and inelastic components from the scattering near structural phase transitions. Pioneering work on $SrTiO_3$ and $KNbO_3$ has been published by Darlington *et al.*[20] We have published our preliminary results on $RbCaF_3$ in a short note by Maetz *et al.*[21] In our experiment the recoilless γ radiation from a 200 mCi ^{57}Co source in a Pd matrix was scattered from a $RbCaF_3$ single crystal and then analyzed by a black absorber of ammonium lithium fluoferrate with an energy resolution of 60 neV. The radiation was detected in a 80-mm^2 Si(Li) detector (resolution 300 eV at 14 keV) which has a favorable peak-to-background ratio and allows the discrimination of fluorescent radiation. In our experimental setup the Si(Li) is fixed in its position, while the source is moving around the 2θ axis. This arrangement avoids microphonic disturbance of the Si(Li) during the measurements. Special care is needed to determine the absorber efficiency P, whose accuracy sensitively involves the error bars of the elastic- and inelastic-scattering intensities. We controlled the spatial homogeneity of the ^{57}Fe concentration, and we avoided demounting of the absorber before finishing a complete run. The efficiency also depends on temperature; therefore, the laboratory is kept air conditioned. In addition we checked that vibrations of external sources (refrigerator and air conditioner) did not generate acoustic noise that shifted the absorber out of resonance.

The elastic I_{el} and inelastic I_{in} intensities from a Bragg reflection are determined from three runs at a given scattering angle: (i) absorber velocity $v = 0$, (ii) absorber velocity $v = \infty$, and (iii) background U with Al absorber in the beam.

$$I_{v=0} = I_{\text{in}} + (1 - P) I_{\text{el}} + U \ ,$$

$$I_{v=\infty} = I_{\text{in}} + I_{\text{el}} + U \ .$$

The absorber efficiency P is determined in the direct beam[12] and defined as $P = (I_{v=0} - I_{v=\infty})/(I_{v=\infty} - U)$, where $I_{v=\infty}$ is the transmitted intensity when the source and the absorber are in relative motion, and $I_{v=0}$ the counting rate when they have no relative motion. U is the background counting rate. The crystal of $RbCaF_3$ was cut with a (311) surface plane; it was polished and tempered at 760 K for 24 hours in order to reduce the concentration of defects at the surface.[20] The active area was 12×8 mm^2, the thickness 2 mm. The mosaic spread was less than 0.2° full width at half maximum (FWHM). The crystal was cooled using a closed-cycle He refrigerator, and its temperature was controlled to ± 0.5 K. The measured elastic intensities from the $\frac{1}{2}(311)_{\text{cubic}}$ superlattice reflection are presented in Fig. 9. Below T_0 our results are in reasonable agreement with the temperature law $I_{\text{el}} \propto (T_0 - T)^{2\beta}$, with β taken from our neutron and x-ray investigations. Of course the statistical accuracy of these experiments here is not sufficient for determining β. On the other hand, the Mössbauer-diffraction experiment has sufficient energy resolution to exclude much of the critical scattering. Domain effects, however, indicating a deviation from the theoretical power law below the critical range, i.e., $T_0 > T > 180$ K are evident in the figure. Above T_0 the measured intensities should be com-

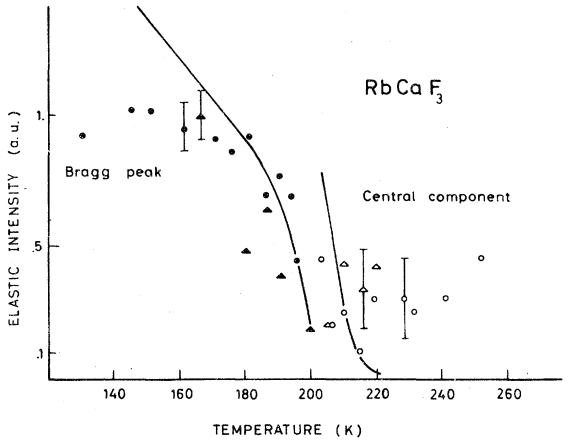

FIG. 9. Elastic intensity from the $\frac{1}{2}(311)_{\text{cubic}}$ superlattice point measured with Mössbauer γ-ray diffraction. The theoretical full lines are discussed in the text.

pared with the central-peak investigation by Rousseau *et al.*[8] These authors determined the characteristic parameters (Γ_0, γ, δ^2, ω_∞^2, and ω_0^2) in the notation of Shapiro *et al.*[19] The elastic intensity I_{el} — with $dE < 60$ neV in our experiment — should follow a law[20]

$$I_{el} \propto \frac{T\delta^2}{\omega_\infty^2 \omega_0^2}, \quad T > T_0 \ .$$

This law does not agree with our results. We have carefully checked that incoherent elastic scattering does not contribute by measuring its intensity two degrees outside the superlattice position. We have also applied γ-ray-induced fluorescent x-ray measurements determining the content of impurity ions. Mg and Cl were indentified with appreciable amount in the ppm range. This might influence the phase-transition temperature reported by Halperin and Varma[22] but we suppose that the major part of the elastic scattering above T_0 results from domains.

The inelastic part of the scattering is presented in Fig. 10. Below T_0 we expect what crystallographers call the thermal diffuse scattering (TDS) from the acoustic phonons beneath the new superlattice Bragg peak mainly. Its temperature dependence should be $I_{in} \propto T(T_0 - T)^{2\beta}$, where the first factor arises from the averaged phonon energy, while the second comes from the inelastic structure factor. We assume the same temperature dependence as for the elastic structure factor. Soft-mode contributions seem to be negligible in this temperature range, since the Rushworth and Ryan[15] Raman studies fo the E_g and A_{1g} modes in the tetragonal phase gave energies that extrapolate to finite values at 200 K, according to the temperature law which they propose. This conclusion is consistent with the fact that the phase transition is slightly first order. However, domain effects are indicated below 180 K in a deviation from the theoretical curve. Above T_0 the inelastic scattering arises from the overdamped soft mode at the R point of the cubic Brillouin zone. The temperature law should read[20] $I_{in} \propto T\omega_\infty^{-2}$, where the quasiharmonic frequency ω_∞ was taken from Almairac *et al.*[1] The soft-mode-induced inelastic scattering seems to be in reasonable agreement with our experiments. Since the inelastic-scattering intensity is proportional to the domain volume distribution of the actual experiment below, but not above, T_0, we do not expect a smooth inelastic-intensity distribution across the phase transition.

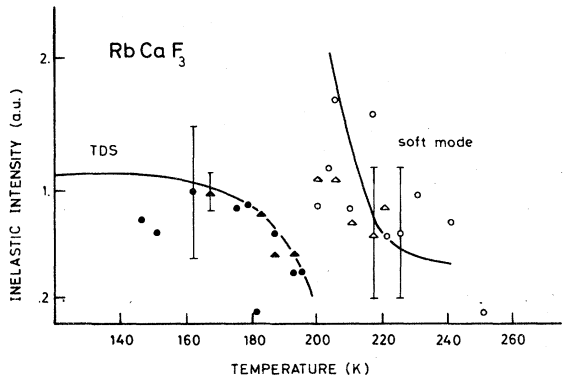

FIG. 10. Inelastic intensity from the $\frac{1}{2}(311)_{cubic}$ superlattice point measured with Mössbauer γ-ray diffraction. The theoretical full lines are discussed in the text.

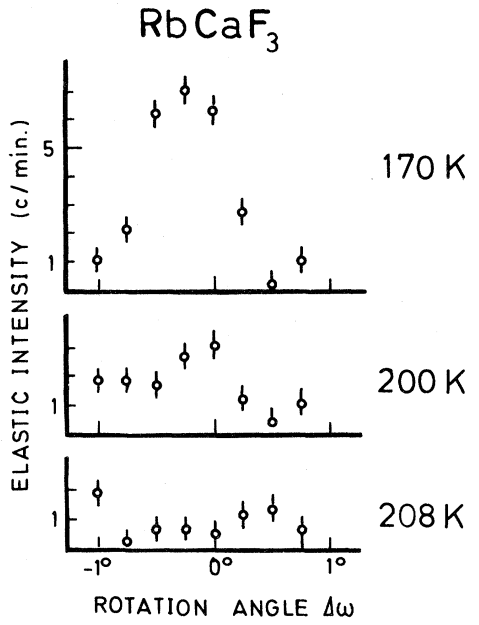

FIG. 11. ω scan from the $\frac{1}{2}(311)_{cubic}$ reflection at three temperatures, showing the growth of the superlattice peak. The elastic ($dE < 60$ neV) data from Mössbauer γ-ray diffraction are plotted.

Figure 11 presents diffraction scans of the elastic intensity ($dE < 60$ neV) taken at three temperatures around T_0. The scans show that in agreement with the x-ray data an elastic line is indicated already above T_0.

V. DISCUSSION

We have investigated the cubic-to-tetragonal phase transition in $RbCaF_3$, applying three different types of diffraction experiments. We obtained the temperature dependence of the order parameter $\langle\varphi\rangle$ unmodified by domains and describe it by a power-law exponent $\beta = 0.25$, where the majority of our data are taken from outside the critical range. This result is consistent with the earlier finding concentrated in the

neighborhood of T_0 from EPR and birefringence experiments by Modine *et al.*,[4] who determined $\beta=0.25$ for $1>T/T_0>0.95$. At lower temperatures $0.95>T/T_0>0.65$, however, they found $\beta=0.33$. In a later paper[2] Bates *et al.* extracted $\beta=0.29$ from the data of the temperature range $1>T/T_0>0.89$, with a T_0 value of 196.9 K. A critical exponent of $\beta=0.25$ is consistent with the neutron scattering data by Rousseau *et al.*[8] and by Kamitakahara *et al.*[9] Very recent birefringence experiments by Kleeman *et al.*[14] on monodomain samples given $\beta=0.28(1)$ in a temperature range 193.6 to 196.6 K. These data can be compared with the EPR result $\beta=0.18(2)$ obtained by Buzare *et al.*[24] in the temperature range 190 to 195.3 K.

Trying to explain our result with a simple picture of the Landau theory leads us to the conclusion that the system is at or near a tricritical point. Starting from the expansion of the free-energy density F in a power series of even powers in $\langle\varphi\rangle$, we obtain

$$F=\sum_{n-1}^{\infty} A_{2n}\langle\varphi\rangle^{2n} f^{(2n)} \ ,$$

where $\langle\varphi\rangle$ is the order parameter, and $f^{(2n)}$ are homogeneous functions of the order $2n$ in the symmetry coefficients $\gamma_i (i=1,2,3)$, characterizing the direction of the rotation axis. We assume $A_2=a(T-T_0)$, $A_4=0$, $A_0>0$, and $A_{2n}=0$ $(n>3)$. The polynomials $f^{(2n)}$ which are relevant are given, for example by Blinc and Žekš[23]

$$f^{(2)}=\gamma_1^2+\gamma_2^2+\gamma_3^2 \ ,$$

$$f^{(6)}=(\gamma_1^2+\gamma_2^2+\gamma_3^2)^3+\alpha(\gamma_1^6+\gamma_2^6+\gamma_3^6)+\beta(\gamma_1^2\gamma_2^2\gamma_3^2) \ .$$

Minimizing the free-energy density F with respect to γ_i $(i=1,2,3,)$ under the constraint $\gamma_1^2+\gamma_2^2+\gamma_3^2=1$ leads to a rotation about one cubic axis, e.g., $\gamma_1=1$, $\gamma_2=0$, $\gamma_3=0$, and the order parameter

$$\langle\varphi\rangle=\left(\frac{a(T_0-T)}{3A_6(1+\alpha)}\right)^{0.25}=\varphi_0(T_0-T)^{0.25} \ .$$

Combining the above results with the free energy and taking φ_0 and T_0 from our experiments, we have evaluated F, which is shown in Fig. 12.

The tricritical character of the phase transition has been confirmed in the EPR studies on uniaxially stressed $RbCaF_3$ in the paper by Buzare *et al.*[24] Unfortunately, due to their experimetnal setup, a [100] stress was applied, which only reduces the number of domains from three to two due to the ratio of the lattice constants $c/a>1$. It was not possible to discriminate between a normal tricritical $(t|\ln t|)^{0.25}$ and a Lifshitz tricritical behavior, where $t=T/T_0$ is the reduced temperature. The Lifshitz-point critical and tricritical behavior in anisotropically stressed

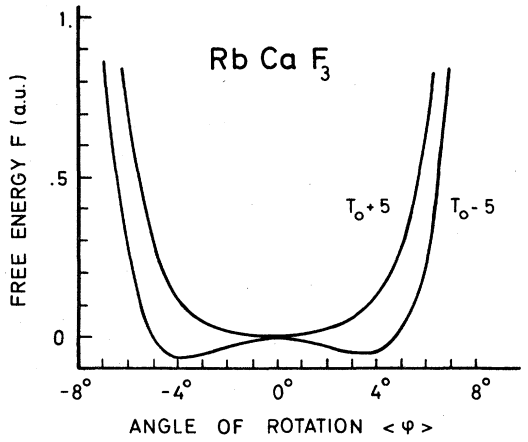

FIG. 12. Free energy of $RbCaF_3$ near the phase-transition point, using the experimental parameters in the power-series expansion of Landau.

perovskites has been theoretically analyzed by Aharony and Bruce[25] leading to a variety of hitherto-unobserved Lifshitz multicritical points. However, for final conclusions to be drawn, more accurate experimental data are needed from $RbCaF_3$. The fluctuations play a central role in these investigations. In order to elucidate this point in more detail including our experimental results, we compare in Table I the anisotropy of the Debye-Waller factors of the fluorines (or the equivalent oxygens), which can be related to the fluctuations of the angle of rotation of the F_6 (or O_6) octahedrons. All data are taken at room temperature. In terms of an angle of rotation we obtain from the component $B_{11}(F)$: $\langle\varphi^2\rangle^{0.5}\cong 5°$ for $RbCaF_3$, which is the largest value in the table. Also the anisotropy is very large.

These conclusions are supported by our measurements of the temperature dependence of the Debye-Waller coefficients for all three atoms. The data are shown in Fig. 5. The temperature dependence turns out to be rather smooth across the phase-transition region except for $B_{11}(F)=B_{22}(F)$. We suppose the

TABLE I. Anisotropic Debye-Waller coefficients $B=8\pi^2\langle u^2\rangle$ of fluorine (oxygen) in the perovskite structure.

Crystal	$B_{11}(A^2)$	B_{11}/B_{33}	T_0(K)	Reference
$KMgF_3$	0.97	5.7	none	Jex *et al.* (Ref.26)
$KMnF_3$	2.72	5.1	176	Meyer *et al.* (Ref. 27)
$RbCaF_3$	3.35	7.4	198	this work
$SrTiO_3$	0.80	2.6	106	Meyer *et al.* (Ref. 27)

Debye-Waller factor to consist of one part which shows a smooth behavior proportional to T (in the high-temperature limit) and a second part which is related to the order-parameter fluctuations concentrated around the soft-mode wave vector in the Brillouin zone. Proceeding this way in the data analysis we obtain after substracting the temperature-proportional part, a well-pronounced peak at T_0. Such a peak was predicted theoretically by Meissner and Binder,[18] and we have been able to see it for the first time in our neutron scattering data. From renormalization-group arguments Meissner and Binder found a temperature dependence of the critical part

$$\langle u^2\rangle_{\text{crit}} \propto \begin{cases} C_0 - C_1^+(t-1)^{1-\alpha} & (T > T_0) \\ C_0 - C_1^-(1-t)^{1-\alpha} - C_2^+(1-t)^{2\beta} & (T \leq T_0) \end{cases} ,$$

where the C coefficients are some constants. At the moment our data do not allow us to extract the critical exponents α and β from the wings above and below T_0, but the peak itself is clearly observed (Fig. 13).

The intimate connection with the EPR linewidth in the slow-motion regime has been pointed out in the paper by Meissner and Binder.[18] In the famous EPR experiment[28] on $SrTiO_3$, the second moment of the linewidth has been found to be proportional to the fluctuation spectrum $I(q,\omega)$ of the staggered rotation coordinate φ_q

$$\langle \delta H^2\rangle \propto \sum_q \int_{-\infty}^{\infty} I(q,\omega)\, d\omega \propto T \sum_q \chi(q,0) \quad .$$

On approaching T_0 a critical slowing down of the fluctuations took place in $SrTiO_3$, and the Fourier components $I(q,\omega)$ of the fluctuation spectrum were concentrated in a peak narrower than the characteristic Larmor frequency of the order 10^8 Hz. In $RbCaF_3$ Buzare *et al.*[24] found no linewidth broadening in their temperature interval of 5 K below T_0.

In our Mössbauer-diffraction experiment the change between a fast-motion regime, where the width of $I(q,\omega)$ exceeds the characteristic resolution energy of the instrument, and the slow-motion regime in the opposite case corresponds to a frequency of 15 MHz. If there is critical slowing down, it should be evident in the inelastic-scattering intensity since

$$I_{\text{in}} \propto \sum_q \int_{\hbar^{-1}\,dE}^{\infty} I(q,\omega)\, d\omega$$

$$\propto T \sum_q \int_{\hbar^{-1}\,dE}^{\infty} \chi''(q,\omega)\frac{d\omega}{\omega} \quad .$$

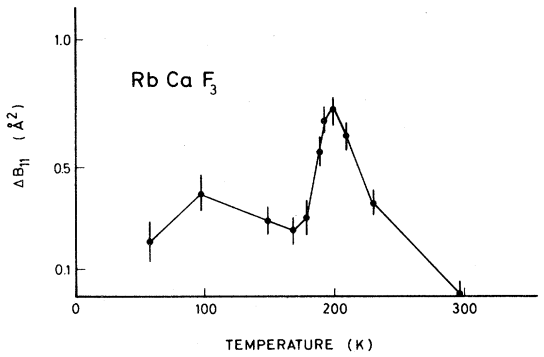

FIG. 13. Peak of the Debye-Waller factor of fluorine obtained from the data of $B_{11}(F) = B_{22}(F)$ after subtracting a smooth part proportional to temperature, which is fixed at 300 and 0 K. The full lines are only guides for the eye.

The elastic intensity should be enhanced due to

$$I_{\text{el}} \propto \sum_q \int_0^{\hbar^{-1}\,dE} I(q,\omega)\, d\omega \quad .$$

We do not observe any effect of this kind, either in the inelastic or in the elastic scattering; a reason may be that critical slowing down affords temperatures closer to T_0. Our inelastic data are in consistent agreement with the inelastic neutron scattering parameters[8] above T_0. However, the elastic part above T_0 deviates. We registrate intensity which is not incoherent elastic as can be checked by an experiment outside the $\frac{1}{2}(311)_{\text{cubic}}$ Bragg position. Obviously a significant part of this scattering must be attributed to domain scattering, probably surface enhanced, which was recognized in our x-ray experiments. Recent investigations of domains in $RbCaF_3$, which we performed on a $5 \times 5 \times 7$-mm^3 brick-shaped single crystal at the high-flux reactor in Grenoble, confirmed the x-ray results on the temperature dependence of the domain volumes. These experiments are not yet finished and will be published elsewhere.

ACKNOWLEDGMENTS

This work was supported by the Bundesministerium für Forschung und Technologie. The authors thank Dr. K. Peters from the Max Planck Institut für Festkörperforschung, Stuttgart, and Dr. N. M. Butt from the Pakistan Institute of Science and Technology, Rawalpindi, Pakistan for valuable discussions.

[1] R. Almairac, M. Rousseau, J. Y. Gesland, J. Nouet, and B. Hennion, J. Phys. (Paris) 38, 1429 (1977).

[2] J. B. Bates, R. W. Major, and F. A. Modine, Solid State Commun. 17, 1347 (1975).

[3] J. C. Ho and W. P. Unruh, Phys. Rev. B 13, 447 (1976).

[4] F. A. Modine, E. Sonder, W. P. Unruh, C. B. Finch, and R. D. Westbrook, Phys. Rev. B 10, 1623 (1974).

[5]J. Berger, G. Hauret, and M. Rousseau, Solid State Commun. 25, 569 (1978).
[6]J. Maetz, M. Müllner, H. Jex, and K. Peters, Solid State Commun. 28, 555 (1978).
[7]C. Ridou, M. Rousseau, J. Y. Gesland, J. Nouet, and A. Zarembowitch, Ferroelectrics 12, 199 (1976).
[8]M. Rousseau, J. Nouet, R. Almairac, and B. Hennion, J. Phys. Lett. (Paris) 37, L33 (1976).
[9]W. A. Kamitakahara and C. A. Rotter, Solid State Commun. 17, 1350 (1975).
[10]H. M. Rietveld, J. Appl. Cryst. 2, 65 (1969).
[11]J. Maetz, thesis (University Frankfurt, 1978) (unpublished).
[12]J. Maetz, M. Müllner, and H. Jex, Phys. Status Solidi A 50, K 117 (1978).
[13]L. E. Halliburton and E. Sonder, Solid State Commun. 21, 445 (1977).
[14]W. Kleemann, F. J. Schäfer, and J. Nouet, (unpublished).
[15]A. J. Rushworth and J. F. Ryan, Solid State Commun. 18, 1239 (1976).
[16]C. Ridou, M. Rousseau, and A. Freund, J. Phys. (Paris) 38, L359 (1977).
[17]J. J. Rousseau, M. Rousseau, and J. C. Fayet, Phys. Status Solidi B 73, 625 (1976).
[18]G. Meissner and K. Bindler, Phys. Rev. B 12, 3948 (1975).
[19]S. M. Shapiro, J. D. Axe, G. Shirane, and T. Riste, Phys. Rev. B 6, 4332 (1972).
[20]C. N. W. Darlington and D. A. O'Connor, J. Phys. C 9, 3561 (1976); and in *Proceedings of the International Conference on Lattice Dynamics, Paris, 1977,* edited by M. Balkanski (Flammarion, Paris, 1977), p. 750.
[21]J. Maetz, N. M. Butt, H. Jex, and M. Müllner, Phys. Lett. A 68, 87 (1978).
[22]B. I. Halperin and C. M. Verma, Phys. Rev. B 14, 4030 (1976).
[23]R. Blinc and B. Žekš, in *Selected Topics in Solid State Physics. Vol. XIII,* edited by E. P. Wohlfarth (North-Holland, Amsterdam, 1974), p. 68.
[24]J. Y. Buzare, J. C. Fayet, W. Berlinger, and K. A. Muller, Phys. Rev. Lett. 42, 465 (1979).
[25]A. Aharony and A. D. Bruce, Phys. Rev. Lett. 42, 462 (1979).
[26]H. Jex and E. Scheich, KfK-Report 2719, Kernforschungszentrum Karlsruhe, 1978) (unpublished), p. 32.
[27]G. M. Meyer, R. J. Nelmes, and J. Hutton, in Ref. 18, p. 652.
[28]K. A. Muller, in *Structural Phase Transition and Soft Modes,* edited by E. J. Samuelsen, E. Anderssen, and J. Feder (Universitetsforlaget, Oslow, 1971), p. 92.